

## 1 **Abstract**

2 Iron (Fe) can limit phytoplankton productivity in approximately 40% of the global  
3 ocean, including high-nutrient, low-chlorophyll (HNLC) waters. However, there is little  
4 information available on the impact of CO<sub>2</sub>-induced seawater acidification on natural  
5 phytoplankton assemblages in HNLC regions. We therefore conducted an on-deck  
6 experiment manipulating CO<sub>2</sub> and Fe using Fe-deficient Bering Sea waters during the  
7 summer of 2009. The concentrations of CO<sub>2</sub> in the incubation bottles were set at 380  
8 and 600 ppm in the non-Fe-added (control) bottles and 180, 380, 600, and 1000 ppm in  
9 the Fe-added bottles. The phytoplankton assemblages were primarily composed of  
10 diatoms followed by haptophytes in all incubation bottles as estimated by pigment  
11 signatures throughout the 5 (controls) or 6 (Fe-added treatments) days incubation period.  
12 At the end of incubation, the relative contribution of diatoms to chlorophyll *a* biomass  
13 was significantly higher in the 380 ppm CO<sub>2</sub> treatment than in the 600 ppm treatment in  
14 the controls, whereas minimal changes were found in the Fe-added treatments. These  
15 results indicate that, under Fe-deficient conditions, the growth of diatoms could be  
16 negatively affected by the increase in CO<sub>2</sub> availability. To further support this finding,  
17 we estimated the expression and phylogeny of *rbcL* (which encodes the large subunit of  
18 RubisCO) mRNA in diatoms by quantitative reverse transcription PCR and clone  
19 library techniques, respectively. Interestingly, regardless of Fe availability, the  
20 transcript abundance of *rbcL* decreased in the high CO<sub>2</sub> treatments (600 and 1000 ppm).  
21 The present study suggests that the projected future increase in seawater *p*CO<sub>2</sub> could  
22 reduce the RubisCO transcription of diatoms, resulting in a decrease in primary  
23 productivity and a shift in the food web structure of the Bering Sea.

24

## 25 **1. Introduction**

26 The atmospheric CO<sub>2</sub> concentration has risen from a pre-industrial level of  
27 approximately 280 ppm to the present level of approximately 400 ppm (WMO, 2013).  
28 Since the industrial revolution, the ocean has absorbed about one-third of CO<sub>2</sub> emitted  
29 by human activity (Sabine et al., 2004). It is predicted that the atmospheric CO<sub>2</sub>  
30 concentration could reach more than 700 ppm by the end of the 21st century (Meehl et  
31 al, 2007), driving a surface seawater pH decrease of 0.3–0.4, the so-called “ocean

32 acidification” (Caldeira and Wickett, 2003). Such a rapid decrease in seawater pH has  
33 most likely not occurred for at least millions of years in the earth’s history (Pearson and  
34 Palmer, 2000). Therefore, it has been suggested that these predicted changes in seawater  
35 carbonate chemistry would have enormous impacts on the health and function of marine  
36 organisms (Raven et al., 2005).

37 In the last decade, numerous studies have been performed to evaluate the impacts of  
38 ocean acidification on marine phytoplankton. In laboratory incubation experiments  
39 using individual species (a single strain), the response of phytoplankton to increased  
40 CO<sub>2</sub> levels differed among phytoplankton species, possibly depending on their ability to  
41 assimilate carbon (Riebesell and Tortell, 2011; Collins et al., 2014). In the natural  
42 environment, these taxon-specific differences in CO<sub>2</sub> response can cause a shift in the  
43 phytoplankton community composition (Engel et al., 2008; Meakin and Wyman, 2011;  
44 Endo et al., 2013) and subsequent changes in ocean trophic structures and  
45 biogeochemical cycles (Riebesell et al., 2007; Yoshimura et al., 2013). However, the  
46 current understanding of the effects of elevated CO<sub>2</sub> on marine phytoplankton is still  
47 insufficient at the community level.

48 In terms of physiology, CO<sub>2</sub> is fixed by the carboxylation enzyme ribulose  
49 bisphosphate carboxylase/oxygenase (RubisCO) in the Calvin-Benson-Bassham (CBB)  
50 cycle. In general, the half-saturation constant of the enzyme ranges between 20 and 70  
51 μmol kg<sup>-1</sup> CO<sub>2</sub> (Badger et al., 1998), whereas the ambient seawater CO<sub>2</sub> levels are  
52 between 10 and 25 μmol kg<sup>-1</sup>. Therefore, the present CO<sub>2</sub> concentration could be  
53 insufficient to ensure effective RubisCO carboxylation. The progression of ocean  
54 acidification could enhance photosynthetic carbon fixation in marine phytoplankton by  
55 increasing CO<sub>2</sub> availability.

56 Recent advances in molecular biology techniques have enabled us to examine the  
57 taxon-specific responses to environmental changes by quantifying functional gene  
58 expression in natural phytoplankton assemblages. For example, John et al. (2007a)  
59 developed a suite of quantitative reverse transcription PCR (qRT-PCR) assays to  
60 quantify *rbcL* (gene encoding the large subunit of RubisCO) mRNA in *Synechococcus*,  
61 haptophytes, and heterokonts including diatoms. John et al. (2007b) demonstrated a  
62 strong negative correlation between diatom-specific *rbcL* mRNA abundance and

63 seawater  $p\text{CO}_2$  in the Mississippi River plume, suggesting that diatoms were  
64 responsible for the greatest drawdown in seawater  $p\text{CO}_2$ . In addition, positive  
65 correlations between diatom-specific *rbcL* transcripts and light-saturated photosynthetic  
66 rates ( $P_{\text{max}}$ ) in seawater were reported (Corredor et al., 2004; John et al., 2007b). These  
67 results suggest that *rbcL* expression in diatoms could be used to estimate the  
68 photosynthetic carbon-fixation capacity of natural phytoplankton assemblages.  
69 Therefore, quantification of clade-specific *rbcL* transcripts can be used to assess the  
70 physiological photosynthetic responses of individual phytoplankton taxa to  
71 environmental changes.

72 The oceanic Bering Sea investigated in this study is an HNLC region (Banse and  
73 English, 1999), where low iron (Fe) availability limits phytoplankton growth and nitrate  
74 utilization, so surface chlorophyll *a* (Chl *a*) concentrations usually remain low in the  
75 summer (Suzuki et al., 2002). Despite the low phytoplankton biomass, the oceanic  
76 domain has the greatest amount of total primary and secondary production in the Bering  
77 Sea (Springer et al., 1996). Suzuki et al. (2002) reported that diatoms were the dominant  
78 phytoplankton group in the oceanic regions of the Bering Sea in the summer. In  
79 addition, Takahashi et al. (2002) showed that diatoms had the greatest contribution in  
80 the sinking particles in the area. However, less is known about the combined effects of  
81 ocean acidification and Fe enrichment on diatoms in such HNLC regions. In addition,  
82 there are no reports on the effects of  $\text{CO}_2$  and Fe availability on *rbcL* transcription of  
83 natural diatom community in HNLC regions.

84 The purpose of this study is to clarify the responses of phytoplankton, especially  
85 diatoms, to  $\text{CO}_2$  enrichment under Fe-depleted and Fe-replete conditions in the Bering  
86 Sea basin using on-deck bottle incubation. Recently, Sugie et al. (2013) reported  
87 changes in phytoplankton biomass and nutrient stoichiometry in this experiment. They  
88 showed that Chl *a* biomass decreased with increased  $\text{CO}_2$  levels only in Fe-depleted  
89 treatments, suggesting that Fe deficiency and increased  $\text{CO}_2$  synergistically reduced the  
90 growth of phytoplankton in the study area. In addition, Yoshimura et al. (2014)  
91 demonstrated that the net production of particulate organic carbon (POC) and total  
92 organic carbon (TOC) decreased under high  $\text{CO}_2$  levels only in the Fe-limited  
93 treatments, whereas those in the Fe-replete treatments were insignificantly different.

94 These studies suggest that the increase in CO<sub>2</sub> could have negative impacts on  
95 phytoplankton growth and/or organic-matter production especially under Fe-depleted  
96 conditions. However, the molecular mechanisms of photosynthetic carbon assimilation  
97 in phytoplankton assemblages were not mentioned in the previous studies. Therefore, in  
98 the present paper, we primarily focused on changes in *rbcL* transcripts in diatoms with  
99 different CO<sub>2</sub> and/or Fe availability.

100

## 101 **2. Materials and Methods**

### 102 **2.1 Experimental setup**

103 The study was carried out aboard the R/V *Hakuho Maru* (JAMSTEC) during the  
104 KH-09-4 cruise in September 2009. The water samples for incubation were collected  
105 from 10 m depth at a station (53° 05' N, 177° 00' W) in the Bering Sea on 9 September  
106 with acid-cleaned Niskin-X bottles attached to a CTD-CMS system. A total of 300 L of  
107 seawater was poured into six 50 L polypropylene carboys through acid-clean silicon  
108 tubing with a 197 µm mesh Teflon net to remove large particles. Subsamples were taken  
109 from each carboy and poured into triplicate acid-cleaned 12 L polycarbonate bottles  
110 (total 18 bottles) for incubation. Initial samples were collected from each carboy. All  
111 sampling was carried out using a trace-metal clean technique to avoid any trace metal  
112 contamination. Prior to incubation, FeCl<sub>3</sub> solutions (5 nmol L<sup>-1</sup> in final concentration)  
113 were added to 12 bottles in order to reduce Fe limitation for the phytoplankton  
114 communities. The CO<sub>2</sub> levels in the incubation bottles were manipulated by injecting  
115 CO<sub>2</sub> controlled dry air purchased from a commercial gas supply company  
116 (Nissan-Tanaka Co., Japan). The air mixtures were passed through 47 mm PTFE filters  
117 (0.2 µm pore size, Millipore) before being added to the incubation bottles. The detailed  
118 procedures for trace metal clean techniques were described in Yoshimura et al. (2013).  
119 The CO<sub>2</sub> concentrations were set at 380 and 600 ppm for the non-Fe-added (control)  
120 bottles (hereafter referred to as 'C-380' and 'C-600', respectively), and 180, 380, 600,  
121 and 1000 ppm for the Fe-added bottles (hereafter referred to as 'Fe-180', 'Fe-380',  
122 'Fe-600', and 'Fe-1000', respectively). Incubation was performed on deck in  
123 temperature-controlled water-circulating tanks for 5 (controls) or 6 (Fe-added  
124 treatments) days at the in situ temperature (8.2°C) and 50% surface irradiance adjusted

125 by natural density screens. The sampling opportunities for each parameter are shown in  
126 Table S1.

127

## 128 **2.2 Carbonate chemistry, nutrients, and Chl *a***

129 The detailed methodology and basic chemical and biological parameters were  
130 reported in Sugie et al. (2013). In brief, during the incubation experiment, samples were  
131 collected from the incubation bottles for dissolved inorganic carbon (DIC), total  
132 alkalinity (TA), nutrients, and Chl *a* determination. DIC and TA concentrations were  
133 measured with a total alkalinity analyzer using the potentiometric Gran plot method  
134 (Kimoto Electric) following Edmond (1970). The levels of  $p\text{CO}_2$  and pH were  
135 calculated from the DIC and TA using the CO2SYS program (Lewis and Wallace,  
136 1998). Concentrations of nitrate plus nitrite, nitrite, phosphate, and silicic acid were  
137 measured using a QuAATro-2 continuous-flow analyzer (Bran+Luebbe). The  
138 concentration of total dissolved Fe (TD-Fe) was determined by a flow-injection method  
139 with chemiluminescence detection (Obata et al., 1993). Chl *a* concentrations were  
140 determined with a Turner Design fluorometer (model 10-AU) with the non-acidification  
141 method (Welschmeyer, 1994).

142

## 143 **2.3 HPLC and CHEMTAX analyses**

144 Samples for high-performance liquid chromatography (HPLC) pigment analysis  
145 were collected on days 3 and 5 for the control treatments and on days 2, 4, and 6 for the  
146 Fe-added treatments. Water samples (400–1000 mL) were filtered onto GF/F filters  
147 under gentle vacuum ( $< 0.013$  MPa) and stored in liquid nitrogen or a deep freezer  
148 ( $-80^\circ\text{C}$ ) until analysis. HPLC pigment analysis was performed following the method of  
149 Endo et al. (2013).

150 To estimate the temporal changes in phytoplankton community structure during  
151 incubation, the CHEMTAX program (MacKey et al., 1996) was used following Endo et  
152 al. (2013). Briefly, optimal initial ratios were obtained following the method of Latasa  
153 (2007). Matrix A was obtained from Suzuki et al. (2002) (Table S2), who examined  
154 phytoplankton community compositions in the Bering Sea. Matrices B, C, and D were  
155 also prepared to determine the optimal pigment/Chl *a* ratios (Table S2). The pigment

156 ratios of Matrices B and C were double and half the Matrix A ratio, respectively. For  
157 Matrix D, values of 0.75, 0.5, and 0.25 for dominant (rank in high pigment/Chl *a* ratio:  
158 1–5), secondary (rank: 6–10), and minor (rank: 11–15) pigments, respectively, were  
159 multiplied by each pigment ratio of Matrix A. We averaged the successive convergent  
160 ratios after the 10 runs among the 4 matrices to identify the most promising initial  
161 pigment ratios. The calculated final pigment/Chl *a* ratios in both the control and  
162 Fe-added treatments (Table S3) were within the range of values reported in Mackey et  
163 al. (1996), Wright and van den Enden (2000), and Suzuki et al. (2002).

164

#### 165 **2.4 qPCR and qRT-PCR**

166 Water samples for DNA and RNA analyses were collected on days 3 and 5 for the  
167 control treatments and on days 2, 4, and 6 for the Fe-added treatments. DNA samples  
168 (400–500 mL) were collected onto 25 mm, 0.2  $\mu\text{m}$  pore size polycarbonate Nuclepore  
169 filters (Whatman) with gentle vacuum ( $< 0.013$  MPa) and stored in liquid nitrogen or a  
170 deep freezer at  $-80^{\circ}\text{C}$  until analysis. DNA extraction was performed following the  
171 method of Endo et al. (2013). Extracted DNA pellets were resuspended in 100  $\mu\text{L}$  of 10  
172 mM Tris-HCl buffer (pH 8.5).

173 For RNA analysis, seawater samples (400–500 mL) were filtered onto 25 mm, 0.2  
174  $\mu\text{m}$  pore size polycarbonate Nuclepore filters (Whatman) with gentle vacuum ( $< 0.013$   
175 MPa) and stored in 1.5 mL cryotubes previously filled with 0.2 g of muffled 0.1 mm  
176 glass beads and 600  $\mu\text{L}$  RLT buffer (Qiagen) with 10  $\mu\text{L mL}^{-1}$   $\beta$ -mercaptoethanol  
177 (Sigma, St Louis, USA). RNA samples were stored in liquid nitrogen or a deep freezer  
178 at  $-80^{\circ}\text{C}$  until analysis. Extraction and purification of RNA samples were performed  
179 using the RNeasy extraction kit (Qiagen) on a vacuum manifold with on-column DNA  
180 digestion using RNase-free DNase (Qiagen) according to the manufacturer's protocol.  
181 RNA was eluted using 50  $\mu\text{L}$  of RNase-free  $\text{H}_2\text{O}$ . Total RNA was then reverse  
182 transcribed into complementary DNA (cDNA) using the PrimeScript<sup>TM</sup> RT reagent Kit  
183 with gDNA Eraser (TaKaRa) following the manufacturer's specifications.

184 Following Smith et al. (2006), we used double-stranded DNA and single-stranded  
185 cDNA standards for DNA and cDNA quantification, respectively. Standard curves for  
186 *rbcL* DNA were generated from plasmid DNA (pUC18, TaKaRa) containing an  
187 artificial gene fragment (113 bp in size) of *rbcL* from the diatom *Thalassiosira*

188 *weissflogii* (CCMP1336). The plasmid DNA was linearized with *Hind*III (TaKaRa) and  
189 quantified using a Thermo NanoDrop spectrophotometer (ND-1000). On the other hand,  
190 to produce the cDNA standard, a PCR-amplified *rbcL* gene fragment of *T. weissflogii*  
191 (CCMP1336) was inserted into a plasmid DNA (pCR2.1, Invitrogen). The plasmid  
192 DNA was purified using the Plasmid maxi kit (Qiagen) and linearized with *Bam*HI  
193 (TaKaRa), and in vitro transcription was performed using T7 RNA polymerase  
194 (Invitrogen) for 2 hours at 37°C with Recombinant RNase Inhibitor (TaKaRa). To  
195 eliminate DNA contamination, RNA was digested for 2 min at 42°C using gDNA  
196 Eraser (TaKaRa). RNA was purified using an RNeasy column (Qiagen) following the  
197 manufacturer's instructions and quantified with a Ribogreen RNA quantification kit  
198 (Molecular Probes) using the manufacturer's standard. RNA was reverse transcribed  
199 into cDNA using the PrimeScript<sup>TM</sup> RT reagent Kit with gDNA Eraser (TaKaRa).

200 Copy numbers of DNA and cDNA standards were calculated using the equation of  
201 Smith et al. (2006), where the molecular mass of each nucleotide (or nucleotide pair) in  
202 double- and single-stranded DNA is assumed to be 660 and 330 Da, respectively. Serial  
203 dilutions of DNA and cDNA standards were prepared using sterilized Milli-Q water.

204 To amplify the *rbcL* gene and cDNA fragments from diatoms, the following specific  
205 primer set designed by John et al. (2007a) was used.

206 Forward primer: 5'-GATGATGARAAAYATTA ACTC-3'

207 Reverse primer: 5'-TAWGAACCTTTWACTTCWCC-3'.

208 Real-time PCR amplification was performed using SYBR Premix Ex Taq II (Perfect  
209 Real Time, TaKaRa) with primer concentrations of 0.4 µM each and a Thermal Cycler  
210 Dice Real Time System (TP800, TaKaRa). Diluted nucleic acid standards were then  
211 added to the PCR mixture. The thermal cycling conditions were 95°C for 60 s, then 40  
212 cycles of 95°C 5 s and 52°C 60 s. The fluorescence intensity of the complex formed by  
213 SYBR green and the double-stranded PCR product was continuously monitored from  
214 cycle 1 to 40. Quantification was achieved by the second-derivative maximum method  
215 (Luu-The et al., 2005), and the copy number for each sample was determined by the  
216 standard curves generated by serial dilutions of the standards.

217

## 218 **2.5 Clone libraries**

219 Clone libraries of *rbcL* cDNA were constructed for the C-380 and C-600 samples on  
220 day 3, and Fe-380 and Fe-600 samples on day 2. The cDNA samples were PCR  
221 amplified with the diatom-specific primer set and thermal cycling condition described  
222 above using the TaKaRa Ex Taq Hot Start Version (TaKaRa). Triplicate PCR products  
223 were mixed and then purified with agarose gel electrophoresis and the PureLink Quick  
224 Gel Extraction Kit (Invitrogen). Purified amplicons from cDNA samples were then  
225 cloned into the pCR2.1 vector using the TOPO TA cloning kit (Invitrogen) following  
226 the manufacturer's instructions. Thirty-five to 50 colonies were randomly picked from  
227 each clone library. Correct cDNA insertions were identified by PCR amplification using  
228 the M13 forward (5'-GTAAAACGACGGCCAG-3') and reverse  
229 (5'-CAGGAAACAGCTATGA-3') primers flanking the cloning site. Plasmid DNA  
230 containing the inserts was cycle-sequenced using the Big Dye Terminator v3.1 Kit  
231 (Applied Biosystems) with the M13 forward primer. The cycle sequencing products  
232 were cleaned by isopropanol precipitation. Sequencing was performed with a 3130  
233 Genetic Analyzer (Life Technologies). The obtained sequences were compared with  
234 *rbcL* sequences deposited in GenBank database (<http://www.ncbi.nlm.nih.gov>) using  
235 the BLAST query engine. Our *rbcL* cDNA sequences were deposited in the DDBJ  
236 database with the following accession numbers: AB985799–AB986033.

237

## 238 **2.6 Phylogenetic and diversity analyses**

239 The *rbcL* sequences obtained were assembled into operational taxonomic units  
240 (OTUs) with > 95% sequence identity, and rarefaction curves were plotted for each  
241 clone library with the software mothur v. 1.27 (Schloss et al., 2009). To estimate OTU  
242 richness, chao1 index (Chao, 1984) values were calculated using the number of  
243 singleton sequences obtained in this study. Genetic diversity was assessed based on the  
244 Shannon-Wiener index ( $H'$ , Shannon, 1948) and Simpson's index ( $D$ , Simpson, 1949).  
245 The statistical significance of differences in the compositions of pairs of *rbcL* sequences  
246 in the libraries was tested using LIBSHUFF (Singleton et al., 2001). The LIBSHUFF  
247 program determined the integral form of the Cramer-von Mises statistic for each pair of  
248 communities using 10,000 randomizations. Any two libraries were considered to be  
249 significantly different from each other if the lower of the significance values generated



250 by the software was  $< 0.025$  ( $p < 0.05$ ).

251

## 252 **2.7 Statistical analysis**

253 Statistical analyses were performed with the program R (<http://www.r-project.org>).  
254 To assess the statistically significant differences between  $p\text{CO}_2$  levels in the control  
255 treatments or between control and Fe treatments, Welch's  $t$ -test was used. Differences  
256 among  $p\text{CO}_2$  levels in the Fe-added treatments were evaluated with Kruskal-Wallis  
257 one-way analysis of variance (ANOVA). Holm's test for multiple comparisons was  
258 used to identify the source of the variance. For all of the analyses, the confidence level  
259 was set at 95% ( $p < 0.05$ ).

260

## 261 **3 Results**

### 262 **3.1 Experimental conditions**

263 The bubbling of  $\text{CO}_2$ -controlled air succeeded in creating significant gradients in  
264  $p\text{CO}_2$ , pH, and DIC in the different  $\text{CO}_2$  treatments except on day 4 in the Fe-added  
265 treatments, when those values did not significantly differ between Fe-380 and Fe-600  
266 (Table 1; Fig. S1). The initial concentrations of nitrate, phosphate, and silicic acid were  
267  $18.06 \pm 0.10$ ,  $1.47 \pm 0.01$ , and  $16.90 \pm 0.12 \mu\text{mol L}^{-1}$ , respectively (Table 1). In the  
268 control bottles, these macronutrients remained until the end of the incubation in both  
269  $\text{CO}_2$  treatments except for silicic acid, which was almost depleted on day 5 in the C-380  
270 treatment (Fig. S2). In the Fe-added bottles, macronutrients were depleted on days 4 or  
271 5 in all  $\text{CO}_2$  treatments (Fig. S2). The TD-Fe concentration was  $1.35 \text{ nmol L}^{-1}$  in the  
272 initial seawater, and it remained low throughout the experiment in the control treatments  
273 (Table 1). In the Fe-added treatments, the TD-Fe concentrations were  $5.50 \pm 0.10 \text{ nmol}$   
274  $\text{L}^{-1}$  in the initial bottles and remained above  $4 \text{ nmol L}^{-1}$  until the end of incubation  
275 (Table 1). The initial Chl  $a$  concentration was  $1.96 \pm 0.14 \mu\text{g L}^{-1}$  (Table 1). In the  
276 control bottles, the Chl  $a$  concentration increased until the end of the incubation and  
277 reached  $10.22 \pm 0.89 \mu\text{g L}^{-1}$  in the C-380 and  $6.28 \pm 0.64 \mu\text{g L}^{-1}$  in the C-600  
278 treatments (Fig. S3). In the Fe-added bottles, the Chl  $a$  concentration increased rapidly  
279 and reached the maximum on day 4 in the Fe-180 and Fe-380 treatments ( $27.51 \pm 0.71$   
280  $\mu\text{g L}^{-1}$  and  $28.45 \pm 3.40 \mu\text{g L}^{-1}$ , respectively) and on day 5 in the Fe-600 and Fe-1000

281 treatments ( $27.68 \pm 0.44 \mu\text{g L}^{-1}$  and  $27.32 \pm 3.05 \mu\text{g L}^{-1}$ , respectively), then declined  
282 toward the end of the incubation (Fig. S3).

283

### 284 **3.2 Phytoplankton pigments**

285 Throughout the experiment, the concentrations of fucoxanthin (Fuco), mainly a  
286 biomarker for diatoms (Ondrusek et al., 1991; Suzuki et al., 2011), and  
287 19'-hexanoyloxyfucoxanthin (19'-Hex), an indicator of haptophytes (Jeffrey and Wright,  
288 1994), were relatively high among the phytoplankton pigments. In the control bottles,  
289 the concentrations of Fuco and 19'-Hex increased over time and reached the maximum  
290 values on day 5 in both the C-380 and C-600 treatments (Figs. 1a and c). After day 3,  
291 the concentrations of Fuco and 19'-Hex were higher in the C-380 treatment than in the  
292 C-600 treatment (day 5: Welch's *t*-test C-380 > C-600,  $p < 0.05$ ), although no statistical  
293 significance was assessed on day 3 because samples were collected from each single  
294 bottle. In the Fe-added bottles, Fuco concentrations increased throughout the incubation  
295 and reached the maximum values on day 6, whereas 19'-Hex concentrations decreased  
296 after day 4 (Figs. 1b and d). The concentrations of Fuco were significantly different  
297 among CO<sub>2</sub> treatments on day 6 (Kruskal-Wallis ANOVA,  $p < 0.05$ ), although these  
298 differences were not supported by multiple comparisons (Holm's test,  $p > 0.05$ ).  
299 Significant differences among CO<sub>2</sub> treatments were also found for the 19'-Hex  
300 concentration on day 6 (Kruskal-Wallis ANOVA,  $p < 0.05$ ), and the values in the  
301 Fe-180 treatment was significantly higher than those in the Fe-1000 treatment (Holm's  
302 test,  $p < 0.05$ ).

303

### 304 **3.3 CHEMTAX outputs**

305 In the initial phytoplankton community, diatoms and haptophytes were the  
306 predominant numbers of the phytoplankton groups (i.e., they contributed 45% and 17%  
307 of the Chl *a* concentration, respectively). The initial contributions of chlorophytes,  
308 cryptophytes, peridinin-containing dinoflagellates, pelagophytes, prasinophytes, and  
309 cyanobacteria to the Chl *a* biomass were 10%, 9%, 8%, 5%, 4%, and 2%, respectively.  
310 In the control bottles, the contributions of diatoms to the Chl *a* biomass increased with  
311 time, and their contributions reached the maximum (70% at the C-380 and 60% at the

312 C-600 treatments) on day 5 (Fig. 2a). On day 5, the contribution of diatoms in the  
313 C-380 treatment was significantly higher than that in the C-600 treatment (Welch's  
314 *t*-test,  $p < 0.05$ ). However, the contribution of haptophytes to the Chl *a* biomass was  
315 higher in the C-600 treatment (21%) than in the C-380 treatment (14%) on day 5  
316 (Welch's *t*-test,  $p < 0.05$ ). Increases in the contributions of diatoms were also observed  
317 in the Fe-added treatment, and the contributions reached the maximum (82–85%) on  
318 day 4 in all CO<sub>2</sub> treatments (Fig. 2b). In terms of diatom contribution, a significant  
319 difference among CO<sub>2</sub> treatments was not detected with Kruskal-Wallis ANOVA ( $p >$   
320 0.05) in the Fe-added bottles. The contributions of haptophytes to Chl *a* biomass did not  
321 differ significantly among CO<sub>2</sub> levels in the Fe-added bottles (Kruskal-Wallis ANOVA,  
322  $p > 0.05$ ).

323

#### 324 **3.4 Expression of diatom *rbcL* gene**

325 A significant linear relationship between the Fuco concentration and the  
326 diatom-specific *rbcL* gene copy number was found (regression analysis:  $r^2 = 0.677$ ,  $p <$   
327 0.001,  $n = 28$ ) in our experiment (Fig. 3). In the control bottles, the transcript abundance  
328 normalized to gene abundance (i.e., cDNA/DNA) of the diatom-specific *rbcL* gene  
329 fragment for the C-380 treatment was significantly higher than that of the C-600  
330 treatment on day 3 (Fig. 4; Welch's *t*-test,  $p < 0.05$ ). In the Fe-added bottles, the  
331 cDNA/DNA ratio of the diatom *rbcL* fragment in the lower CO<sub>2</sub> treatments (Fe-180 and  
332 Fe-380) was higher than that in the Fe-600 treatment on day 2 (Fig. 4; Holm's test,  $p <$   
333 0.05).

334

#### 335 **3.5 Clone libraries of diatom *rbcL* cDNA**

336 Rarefaction curves were plotted for the *rbcL* cDNA libraries (Fig. 5). In terms of  
337 unique taxa, the highest number of OTUs was found in the C-380 treatment (Table 2).  
338 The highest chao1 value was found in the C-600 treatment, whereas the lowest value  
339 was found in the Fe-600 treatment. Shannon-Wiener and Simpson diversity indices  
340 revealed that the cDNA libraries in the 380 ppm CO<sub>2</sub> bottles were more diverse than  
341 those in the 600 ppm CO<sub>2</sub> bottles in both the control and Fe-added treatments, although  
342 the values were not statistically significant between CO<sub>2</sub> treatments (*t*-test,  $p > 0.05$ )

343 (Table 2).

344 All sequences obtained from the cDNA libraries were more than 95% similar to  
345 sequences deposited in the GenBank. These sequences could be classified into the  
346 following 11 phylogenetic groups: Chaetocerotaceae, Coscinodiscaceae,  
347 Cymatosiraceae, Stephanodiscaceae, Thalassiosiraceae, unidentified centrics,  
348 Bacillariaceae, Naviculaceae, Fragillariaceae, unidentified pennates, and other  
349 eukaryotes by comparison with known *rbcL* sequences from GenBank. Sequences that  
350 could not be classified into a specific diatom family (e.g., closely related to two or more  
351 diatom families with same similarity score) were assigned as unidentified centrics or  
352 unidentified pennates. Other eukaryotes consisted of haptophytes, pelagophytes,  
353 dictyochophytes, dinoflagellates, and diatoms which could not be assigned to centrics  
354 and pennates. For all of the cDNA libraries, more than 88% of *rbcL* sequences were  
355 most closely affiliated with those of cultured diatoms. In the initial cDNA library, the  
356 most abundant sequences were closely affiliated with the diatom family Bacillariaceae  
357 (46%), followed by other eukaryotes and Cymatosiraceae (17% and 14%, respectively)  
358 (Fig. 6). The contributions of other diatom groups were less than 6% in the initial clone  
359 library. In the control bottles, the contributions of Coscinodiscaceae increased to 12–  
360 14%, whereas those of Cymatosiraceae decreased to 4%. In the Fe-added bottles, the  
361 contributions of Chaetocerotaceae and unidentified centrics to the total increased to  
362 more than 8% and 20%, respectively. In contrast, the contributions of Bacillariaceae  
363 decreased below 24% in both the Fe-380 and Fe-600 treatments.

364 Statistic analysis using LIBSHUFF revealed that the cDNA libraries in the control  
365 treatments were not significantly different from the initial sample regardless of the CO<sub>2</sub>  
366 level, whereas those in the Fe-added bottles differed significantly from the initial  
367 assemblage (LIBSHUFF,  $p < 0.05$ ) (Table 3). No significant difference in the cDNA  
368 library was found between C-380 and C-600 treatments in the control bottles  
369 (LIBSHUFF,  $p > 0.05$ ). However, a significant difference between the Fe-380 and  
370 Fe-600 treatments was detected in the Fe-added bottles (LIBSHUFF,  $p < 0.05$ ). In  
371 addition, cDNA libraries in the Fe-added bottles differed significantly from those of the  
372 control bottles in both the Fe-380 and Fe-600 treatments (LIBSHUFF,  $p < 0.05$ ).

373

## 374 **4 Discussion**

### 375 **4.1 Changes in phytoplankton community structure during incubation**

376 Our CHEMTAX analysis suggested that the diatoms were the principal contributors  
377 to the Chl *a* biomass in the initial phytoplankton community, followed by haptophytes  
378 (Fig. 2). The results were consistent with those reported by Suzuki et al. (2002), who  
379 examined the community structure in the Bering Sea during early summer of 1999.  
380 These results suggest that diatoms and haptophytes are ecologically important  
381 phytoplankton groups in the study area during the summer. Compared with previous  
382 reports in the area (Suzuki et al., 2002; Yoshimura et al., 2013), a relatively high initial  
383 Chl *a* concentration was observed in our experiment, possibly due to an intrusion of the  
384 coastal seawater mass from the Aleutian trenches (Sugie et al., 2013). However, the Fe  
385 infusion induced significant increases in Chl *a* biomass and concomitant rapid  
386 drawdowns of macronutrients in our incubation bottles (Fig. S2). This indicates that the  
387 seawater used for the incubation was Fe-limited for phytoplankton assemblages. Our  
388 HPLC and CHEMTAX results suggested that the increase in phytoplankton biomass  
389 was mainly due to an increase in diatoms (Figs. 1b and 2b).

390 We found that the growth of Fuco was less in the high CO<sub>2</sub> bottles in the control  
391 treatments (Fig. 1a), suggesting that the elevated CO<sub>2</sub> levels could have a negative  
392 impact on the diatom biomass in the study area. Negative effects on diatoms induced by  
393 an increase in CO<sub>2</sub> availability were also reported in field incubation experiments  
394 conducted in the Bering Sea and the Okhotsk Sea (Hare et al., 2007 and Yoshimura et  
395 al., 2010, respectively). However, such trends have rarely been observed in other  
396 regions of the world's oceans (e.g., Tortell et al., 2002; Kim et al., 2006; Feng et al.,  
397 2009; Hoppe et al., 2013; Endo et al., 2013). Therefore, the responses of phytoplankton  
398 assemblages to ocean acidification can differ among geographic locations due to the  
399 differences in the biogeography of phytoplankton and/or environmental conditions.

400 One possible cause of the geographic specificity in the open Bering Sea is the  
401 differences in the species composition of diatoms. Our microscope data showed that  
402 centric diatoms such as Chaetocerataceae and Rhizosoreniaceae were predominant at  
403 the beginning of the incubation in terms of carbon biomass, and the coastal diatom  
404 species *Chaetoceros* spp. became predominant in all incubation bottles after day 2  
405 (Sugie et al., 2013). Therefore, the relative decrease in Fuco biomass with increased

406 CO<sub>2</sub> levels might be partially explained by the decrease in *Chaetoceros* spp. A previous  
407 field incubation experiment conducted in the Bering Sea also showed that the carbon  
408 biomass of the *Chaetoceros* spp. decreased at higher CO<sub>2</sub> levels (600–960 μatm CO<sub>2</sub>),  
409 although it increased at 1190 μatm CO<sub>2</sub> (Yoshimura et al., 2013). However, Tortell et al.  
410 (2008) demonstrated that relative abundance of *Chaetoceros* spp. increased under  
411 elevated CO<sub>2</sub> levels in the Ross Sea. In the previous laboratory culture experiments, the  
412 effects of increased CO<sub>2</sub> on the growth and/or photosynthesis of *Chaetoceros* spp. were  
413 also inconsistent. For example, Ihnken et al. (2011) demonstrated that the growth of  
414 diatom *Chaetoceros muelleri* decreased with elevated CO<sub>2</sub> (decreased pH) levels  
415 although their photosynthetic capacity increased. In contrast, Trimborn et al. (2013)  
416 showed a significant increase in the growth rate of *Chaetoceros debilis* under high CO<sub>2</sub>  
417 condition. In addition, no CO<sub>2</sub>-related change in the growth and photosynthetic  
418 physiology of *Chaetoceros brevis* was found (Boelen et al., 2011). These results suggest  
419 that the responses to elevated CO<sub>2</sub> differ among *Chaetoceros* species.

420 The concentrations of 19'-Hex were significantly lower in the C-600 treatment than  
421 those in the C-380 treatment (Fig. 1c), suggesting that the ocean acidification could  
422 induce negative effects not only on the biomass of diatoms, but also on that of  
423 haptophytes in the study area. Similar results were obtained from the previous field  
424 studies in other regions (e.g., Feng et al., 2010; Endo et al., 2013). One possible factor  
425 underlying these decreases is that the reduced carbonate-saturation states under high  
426 CO<sub>2</sub> conditions. The energetic cost of calcification in coccolithophores will increase  
427 with a decrease in pH (Mackinder et al., 2010). Therefore, additional energy might be  
428 needed for cell growth in seawater with high CO<sub>2</sub> levels. In addition, non-calcifying  
429 haptophytes such as *Phaeocystis* spp. often dominate among haptophytes in the natural  
430 phytoplankton community (Schoemann et al., 2005), although the effects of ocean  
431 acidification on them are still not well understood. Therefore, additional study using a  
432 wide range of haptophyte species would be required for a detailed understanding of the  
433 responses of the haptophyte community to CO<sub>2</sub>-induced ocean acidification.

434 Our CHEMTAX outputs showed that the relative contributions of diatoms decreased  
435 with increased CO<sub>2</sub> levels, whereas the contributions of haptophytes increased in both  
436 the control and Fe-added bottles (Fig. 2). This indicates that the negative impacts of  
437 increased CO<sub>2</sub> on diatoms were greater than those on haptophytes and other

438 phytoplankton groups. Another possibility is that the competitions between diatoms and  
439 other phytoplankton taxa could occur. For example, diatoms could become less  
440 competitive when silicic acid is exhausted, because Si-depletion significantly depressed  
441 the growth and could induce their cell death (Harrison et al., 1977; Jiang et al. 2014).  
442 However, concentrations of silicic acid were not significantly different among CO<sub>2</sub>  
443 levels in the Fe-added treatments (Fig. S2f). Moreover, in the control treatments, silicic  
444 acid was almost depleted in the low CO<sub>2</sub> treatment after day 5 but not in the high CO<sub>2</sub>  
445 treatment (Fig. S2e). These results suggest that availability of silicic acid little affected  
446 the decreases in relative diatom contribution to Chl *a* biomass. Larger diatoms can  
447 contribute to efficient transfer of energy and organic compounds to higher trophic levels  
448 because they would create a shorter food chain compared with nano- and pico-sized  
449 phytoplankton (Michaels and Silver, 1988). Because diatoms form a large part of  
450 phytoplankton biomass in the Bering Sea basin (Suzuki et al., 2002; Takahashi et al.,  
451 2002), the decrease in the relative contribution of diatoms with increasing CO<sub>2</sub> could  
452 reduce the energy transferred from the primary producers to the higher trophic levels.

453 The decreases in Fuco growth and relative contribution of diatoms were larger in the  
454 control bottles than those in the Fe-added treatments (Figs. 1 and 2), suggesting that the  
455 negative effect of CO<sub>2</sub> enrichment was greater in the Fe-limited conditions. These  
456 results are consistent with Sugie et al. (2013) and Yoshimura et al. (2014), who  
457 observed significant decreases in diatom carbon biomass and particulate organic carbon  
458 (POC) production under high CO<sub>2</sub> levels in the control treatments, whereas those were  
459 insignificantly changed in the Fe-added treatments. Sugie et al. (2013) indicated that the  
460 Fe limitations for phytoplankton in the control bottles were enhanced at high CO<sub>2</sub> levels,  
461 likely due to the reduction of Fe bioavailability as reported in Shi et al. (2010). The  
462 combined effects of CO<sub>2</sub> and Fe availability were also tested in a diatom-dominated  
463 phytoplankton community in the Southern Ocean (Hoppe et al., 2013). In their study,  
464 net primary productivity in seawater decreased with increased *p*CO<sub>2</sub> levels in the  
465 Fe-depleted treatments but not in the Fe-enriched treatments. These studies indicate that  
466 an interactive effect of CO<sub>2</sub> enrichment and Fe limitation could occur in the  
467 diatom-dominated natural phytoplankton assemblages in the HNLC region.

468

## 469 **4.2 *rbcL* expression in diatoms**

470 A significant correlation between diatom *rbcL* copies per liter and Fuco  
471 concentration was found in this study (Fig. 3), suggesting the usefulness of the *rbcL*  
472 gene fragment as a proxy for diatoms. In addition, the cDNA sequences obtained from  
473 cloning were dominated by the diatom-derived *rbcL* gene (Fig. 6). These results  
474 indicate that the *rbcL* primers used successfully and selectively amplified the *rbcL* gene  
475 of diatoms. Suzuki et al. (2011) showed that Fuco concentration significantly correlated  
476 with diatom carbon biomass in the subarctic Pacific. Furthermore, Matsuda et al. (2011)  
477 showed that the number of *rbcL* gene per cell varies among diatom species, and it was  
478 positively correlated with cell size. Therefore, we concluded that the *rbcL* gene could  
479 serve as a potential molecular marker for diatom biomass.

480 The transcript abundance of the diatom-specific *rbcL* gene decreased with elevated  
481 CO<sub>2</sub> levels in both the control and Fe-added treatments (Fig. 4). Because RubisCO  
482 expression is primarily controlled at the transcriptional level in the natural  
483 phytoplankton community (Xu and Tabita, 1996; Wawrik et al., 2002), our results  
484 suggest that increased CO<sub>2</sub> levels could reduce the amount of RubisCO in diatoms. It  
485 should be noted that significant decreases in *rbcL* expression with increased CO<sub>2</sub> levels  
486 were observed on days 2 or 3, when macronutrients still remained (Fig. S2). This  
487 indicates that the downregulation of *rbcL* expression in diatoms was probably caused by  
488 the increase in CO<sub>2</sub> availability. It has been shown that some land plants can increase  
489 their nitrogen utilization efficiency under elevated CO<sub>2</sub> levels by reducing the  
490 investment of nitrogen in RubisCO (Curtis et al., 1989; Makino et al., 2003). Losh et al.  
491 (2012; 2013) also demonstrated a decreased RubisCO contribution to the total protein in  
492 the California Current phytoplankton community with an increase in CO<sub>2</sub> level.  
493 Because a decrease in the expression of RubisCO can result in a reduction of the  
494 potential capacity for carbon fixation in the natural environment (John et al., 2007b),  
495 our results indicate that an increase in CO<sub>2</sub> levels could have a negative impact on  
496 photosynthetic carbon fixation for diatoms in the study area. Recently, Gontero and  
497 Salvucci (2014) pointed out that RubisCO activase plays a key role in the modification  
498 of RubisCO activity, and consequently in the capacity of carbon fixation, although the  
499 occurrence of RubisCO activase in diatoms is not well understood. Further studies must  
500 be needed for better understanding of the impacts of elevated CO<sub>2</sub> on photosynthetic



501 physiology in diatoms.

502 The negative effects of increasing CO<sub>2</sub> on diatom biomass were not severe in the  
503 Fe-added bottles relative to Fe-limited control bottles (Figs. 1a and b), whereas *rbcL*  
504 transcripts decreased with increased CO<sub>2</sub> regardless of Fe availability (Fig. 4). This  
505 suggests that the diatoms could overcome the decrease in RubisCO activity in the  
506 Fe-added treatments. According to our cloning data (Fig. 6), a shift in phylogenetic  
507 composition of the diatoms actively transcribed *rbcL* was observed in the Fe-added  
508 bottles. In addition,  $F_v/F_m$  values increased significantly with Fe enrichment in our  
509 incubation experiments (Sugie et al., 2013), indicating an increase in the photochemical  
510 quantum efficiency of photosystem II for the diatoms. Therefore, the photosystem II  
511 activity might compensate for the decrease in RubisCO expression under Fe-replete  
512 conditions.

513 It is generally recognized that phytoplankton autonomously regulate the transcription  
514 of the *rbcL* gene in response to environmental conditions such as light and nutrient  
515 availability (Pichard et al., 1996; Granum et al., 2009; John et al., 2010). However, the  
516 mechanisms controlling the transcription of RubisCO operon in diatoms are largely  
517 unknown. Recently, Minoda et al. (2010) showed that the red alga *Cyanidioschyzon*  
518 *merolae* increased *rbcL* transcription at high levels of NADPH, 3-phosphoglyceric acid  
519 (3-PGA), or ribulose-1,5-bisphosphate (RuBP) under the influence of the transcription  
520 factor Ycf30. In addition, it has been reported that regeneration of RuBP could be a  
521 limiting factor for the CBB cycle in high CO<sub>2</sub> conditions (von Caemmerer and Farquhar,  
522 1981; Stitt, 1991; Onoda et al., 2005). Thus, one possible mechanism underlying the  
523 reduction of diatom *rbcL* transcripts observed in our study is related to a decrease in  
524 RuBP concentration in the chloroplasts due to the increase in CO<sub>2</sub> availability for  
525 diatoms. Because diatoms possess the same type of RubisCO (Form ID) and gene  
526 homologs encoding the Ycf30 protein (i.e., *ycf30*) (Kowallik et al., 1995), they could  
527 control *rbcL* gene expression using the same mechanisms as *C. merolae*. Further studies  
528 using marine diatom cultures are required to obtain a better understanding of the  
529 physiological mechanisms controlling the expression of RubisCO.

530 In our experiment, the rarefaction curves plateaued to some extent in all treatments  
531 (Fig. 5), indicating that the clone numbers screened from each library were statistically

532 sufficient for further diversity analysis. Taxonomic compositions in the cDNA library  
533 were considerably different from those in the diatom carbon biomass revealed by  
534 microscopic analysis by Sugie et al. (2013), which were composed primarily by  
535 Chaetocerataceae. This implies that the predominant diatoms did not necessarily  
536 become transcriptionally active *rbcL* phylotypes in our experiment. In addition, because  
537 16–42% of the sequences were classified as unidentified diatoms or other eukaryotes,  
538 the primer set used in this study might be insufficient to estimate diatom composition at  
539 the family level.

540 The *rbcL* cDNA libraries in the Fe-added treatments differed significantly from the  
541 initial library, whereas those in the control treatments were not significantly different  
542 (Table 3), suggesting that the diatom blooms induced by Fe infusion were associated  
543 with the change in the relative contribution of *rbcL* expression in diatoms. For example,  
544 compared to the initial seawater, the relative contributions of Chaetocerataceae and  
545 unidentified centrics to the *rbcL* cDNA library increased markedly in the Fe-added  
546 bottles whereas they remained minor components in the control bottles (Fig. 6). This  
547 indicates that the relative significance of the RubisCO activity of these phylotypes could  
548 be increased by Fe enrichment. In addition, cDNA libraries were significantly different  
549 from each other at different CO<sub>2</sub> levels in the Fe-added bottles (Table 3). This indicates  
550 that the transcriptionally active phylotypes in diatoms could shift in response to an  
551 increase in the CO<sub>2</sub> level. On the other hand, the diversity indices for the  
552 diatom-specific *rbcL* cDNA sequences were not affected by CO<sub>2</sub> availability (Table 2).  
553 In addition, the highest chao1 (richness) value was observed in C-600 treatment. These  
554 results suggest that the richness and/or diversity of diatom phylotypes actively  
555 transcribing *rbcL* gene could remain under elevated CO<sub>2</sub> levels.

556

## 557 **5 Conclusions**

558 The present study showed that an increase in CO<sub>2</sub> levels could have negative impacts  
559 on diatom biomass in the Bering Sea, especially under Fe-limited conditions. Because  
560 diatoms play pivotal roles in carbon sequestration and food webs in the Bering Sea  
561 (Springer et al., 1996; Takahashi et al., 2002), our results indicate that ocean  
562 acidification might alter the biogeochemical processes and ecological dynamics in the

563 study area. Although the present results cannot be extrapolated to other HNLC  
564 ecosystems due to differences in other environmental conditions, our findings suggest  
565 that the combined effects of CO<sub>2</sub> and other environmental factors such as Fe availability  
566 need to be examined for a better understanding of the potential impacts of ocean  
567 acidification on marine ecosystems.

568 We examined, for the first time, the relationships between CO<sub>2</sub> levels or Fe  
569 availability and RubisCO expression of diatoms in the Bering Sea. Significant decreases  
570 in the *rbcL* expression of diatoms were observed at elevated CO<sub>2</sub> levels in both the  
571 Fe-limited and Fe-enriched treatments, suggesting that ocean acidification could reduce  
572 the primary productivity in the study area. Our results indicate that the amount of *rbcL*  
573 transcripts could be an important indicator to assess the physiological responses of  
574 RubisCO activity in diatoms to environmental drivers. However, photosynthetic carbon  
575 fixation in diatoms can be controlled not only by RubisCO activity, but also other  
576 processes such as carbon concentrating mechanisms (CCMs) and/or RuBP regeneration  
577 (Rost et al., 2003; Onoda et al., 2005). More detailed studies on molecular mechanisms  
578 are required to clarify the physiological responses of the diatom community to CO<sub>2</sub> and  
579 Fe availability.

580

## 581 **6 Acknowledgements**

582 We thank the captain, officers, and crew of the R/V *Hakuho Maru* for their great  
583 support and field assistance. We also thank J. Nishioka for Fe analysis. We also  
584 appreciate the editor and three referees for providing constructive comments on the  
585 manuscripts. This work was conducted within the framework of the Plankton  
586 Ecosystem Response to CO<sub>2</sub> Manipulation Study (PERCOM) and was partly supported  
587 by the grants from CRIEPI (#090313) and Grant-in-Aid for Scientific Research  
588 (#18067008, #22681004).

589

## 590 **7 References**

591 Badger, M. R., Whitney, S. M., Ludwig, M., Yellowlees, D. C., Leggat, W., and Price,  
592 G. D.: The diversity and co-evolution of RubisCO, plastids, pyrenoids, and  
593 chloroplast based CO<sub>2</sub>-concentrating mechanisms in algae, *Can. J. Bot.*, 76, 1052–

- 594 1071, 1998.
- 595 Banse, K., and English, D. C.: Comparing phytoplankton seasonality in the eastern and  
596 western subarctic Pacific and the western Bering Sea, *Prog. Oceanogr.*, 43, 235–  
597 288, 1999.
- 598 Boelen, P., van de Poll, W. H., van de Strate, H. J., Neven, I. A., Beardall, J., Buma, A.  
599 G. J.: Neither elevated nor reduced CO<sub>2</sub> affects the photophysiological  
600 performance of the marine Antarctic diatom *Chaetoceros brevis*, *J. Exp. Mar. Biol.*  
601 *Ecol.*, 406, 38–45, 2011.
- 602 Caldeira, K., and Wickett, M. E.: Anthropogenic carbon and ocean pH. *Nature*, 425,  
603 365, 2003.
- 604 Chao, A.: Nonparametric estimation of the number of classes in a population. *Scand. J.*  
605 *Stat.*, 265–270, 1984.
- 606 Collins, S., Rost, B., and Rynearson, T. A.: Evolutionary potential of marine  
607 phytoplankton under ocean acidification, *Evol. Appl.*, 7, 140–155, 2014.
- 608 Corredor, J. E., Wawrik, B., Paul, J. H., Tran, H., Kerkhof, L., Lopez, J. M., Dieppa, A.,  
609 and Cardenas, O.: Geochemical rate-RNA integrated study:  
610 ribulose-1,5-bisphosphate carboxylase/oxygenase gene transcription and  
611 photosynthetic capacity of planktonic photoautotrophs, *Appl. Environ. Microbiol.*,  
612 70, 5459–5468, 2004.
- 613 Curtis, P. S., Drake, B. G., and Whigham, D. F.: Nitrogen and carbon dynamics in C<sub>3</sub>  
614 and C<sub>4</sub> marsh plants grown under elevated CO<sub>2</sub> in situ, *Oecologia*, 78, 297–301,  
615 1989.
- 616 Edmond, J. M.: High precision determination of titration alkalinity and total carbon  
617 dioxide content of sea water by potentiometric titration, *Deep-Sea Res.*, 17, 737–  
618 750, 1970.
- 619 Endo, H., Yoshimura, T., Kataoka, T., and Suzuki, K.: Effects of CO<sub>2</sub> and iron  
620 availability on phytoplankton and eubacterial community compositions in the  
621 northwest subarctic Pacific, *J. Exp. Mar. Biol. Ecol.*, 439, 160–175, 2013.
- 622 Engel, A., Schulz, K. G., Riebesell, U., Bellerby, R., Delille, B., Schartau, M.: Effects  
623 of CO<sub>2</sub> on particle size distribution and phytoplankton abundance during a  
624 mesocosm bloom experiment (PeECE II), *Biogeosciences*, 5, 509–521, 2008.
- 625 Feng, Y., Hare, C. E., Leblanc, K., Rose, J. M., Zhang, Y., DiTullio, G. R., Lee, P. A.,  
626 Wilhelm, S. W., Rowe, J. M., Sun, J., Nemcek, N., Gueguen, C., Passow, U.,  
627 Benner, I., Brown, C., and Hutchins, D. A.: Effects of increased pCO<sub>2</sub> and  
628 temperature on the North Atlantic spring bloom. I. The phytoplankton community  
629 and biogeochemical response, *Mar. Ecol. Prog. Ser.* 388, 13–25, 2009.
- 630 Feng, Y., Hare, C. E., Rose, J. M., Handy, S. M., DiTullio, G. R., Lee, P. A., Smith Jr,  
631 W. O., Peloquin, J., Tozzi, S., Sun, J., Zhang, Y., Dunbar, R. B., Long, M. C.,  
632 Sohst, B., Lohan, M., and Hutchins, D. A.: Interactive effects of iron, irradiance

- 633 and CO<sub>2</sub> on Ross Sea phytoplankton, *Deep-Sea Res. I*, 57, 368–383, 2010.
- 634 Gontero, B., and Salvucci, M. E.: Regulation of photosynthetic carbon metabolism in  
635 aquatic and terrestrial organisms by Rubisco activase, redox-modulation and  
636 CP12, *Aquat. Bot.*, 118, 14–23, 2014.
- 637 Granum, E., Roberts, K., Raven, J. A., Leegood, R. C.: Primary carbon and nitrogen  
638 metabolic gene expression in the diatom *Thalassiosira pseudonana*  
639 (Bacillariophyceae): Diel periodicity and effects of inorganic carbon and nitrogen,  
640 *J. Phycol.*, 45, 1083–1092, 2009.
- 641 Hare, C. E., Leblanc, K., DiTullio, G. R., Kudela, R. M., Zhang, Y., Lee, P. A.,  
642 Riseman, S., and Hutchins, D. A.: Consequences of increased temperature and  
643 CO<sub>2</sub> for phytoplankton community structure in the Bering Sea, *Mar. Ecol. Prog.  
644 Ser.*, 352, 9–16, 2007.
- 645 Harrison, P.J., Conway, H.L., Holmes, R.W., and Davis, C.O.: Marine diatoms grown  
646 in chemostats under silicate or ammonium limitation. III. Cellular chemical  
647 composition and morphology of *Chaetoceros debilis*, *Skeletonema costatum*, and  
648 *Thalassiosira gravida*, *Mar. Biol.*, 43(1), 19–31, 1977.
- 649 Hoppe, C. J., Hassler, C. S., Payne, C. D., Tortell, P. D., Rost, B. and Trimborn, S.: Iron  
650 limitation modulates ocean acidification effects on Southern Ocean phytoplankton  
651 communities, *PloS One*, 8(11), e79890, 2013.
- 652 Ihnken, S., Roberts, S., and Beardall, J.: Differential responses of growth and  
653 photosynthesis in the marine diatom *Chaetoceros muelleri* to CO<sub>2</sub> and light  
654 availability, *Phycologia*, 50, 182–193, 2011.
- 655 Jeffrey, S.W., and Wright, S.W.: Photosynthetic pigments in the Haptophyta, in: *The*  
656 *Haptophyte algae*, Green, J. C., and Leadbeater, B. S. C. (Eds.), Carendon Press,  
657 Oxford, 111–132, 1994.
- 658 Jiang, Y., Yin, K., Berges, J.A., and Harrison, P.J.: Effects of silicate resupply to  
659 silicate-deprived *Thalassiosira weissflogii* (Bacillariophyceae) in stationary or  
660 senescent phase: short-term patterns of growth and cell death, *J. Phycol.*, 50(3),  
661 602–606, 2014
- 662 John, D. E., Jose, López-Díaz, J. M., Cabrera, A., Santiago, N. A., Corredor, J. E.,  
663 Bronk, D. A., and Paul, J. H.: A day in the life in the dynamic marine  
664 environment: how nutrients shape diel patterns of phytoplankton photosynthesis  
665 and carbon fixation gene expression in the Mississippi and Orinoco River plumes,  
666 *Hydrobiologia*, 679, 155–173, 2010.
- 667 John, D. E., Patterson, S. S., and Paul, J. H.: Phytoplankton group specific quantitative  
668 polymerase chain reaction assays for RuBisCO mRNA transcripts in seawater,  
669 *Mar. Biotechnol.*, 9, 747–759, 2007a.
- 670 John, D. E., Wang, Z. A., Liu, X. W., Byrne, R. H., Corredor, J. E., Lopez, J. M.,  
671 Cabrera, A., Bronk, D. A., Tabita, F. R., and Paul, J. H.: Phytoplankton carbon  
672 fixation gene (RuBisCO) transcripts and air-sea CO<sub>2</sub> flux in the Mississippi River

- 673 plume, *ISME J.*, 1, 517–531, 2007b.
- 674 Kim, J. -M., Lee, K., Shin, K., Kang, J. -H., Lee, H. -W., Kim, M., Jang, P. -G., and  
675 Jang, M. -C.: The effect of seawater CO<sub>2</sub> concentration on growth of the natural  
676 phytoplankton assemblage in a controlled mesocosm experiment, *Limnol.*  
677 *Oceanogr.*, 51, 1629–1636, 2006.
- 678 Kowallik, K. V., Stoebe, B., Schaffran, I., KrothPancic, P., and Freier, U.: The  
679 chloroplast genome of a chlorophyll *a+c*-containing alga, *Odontella sinensis*,  
680 *Plant Mol. Biol. Rep.*, 13, 336–342, 1995.
- 681 Latasa, M.: Improving estimations of phytoplankton class abundances using  
682 CHEMTAX, *Mar. Ecol. Progr. Ser.*, 329, 13–21, 2007.
- 683 Lewis, E., and Wallance, D. W. R.: Program developed for CO<sub>2</sub> system calculations.  
684 ORNL/CDIAC-105. Carbon dioxide information analysis center, Oak Ridge  
685 National Laboratory, US Department of Energy, Oak Ridge, Tennessee, 1998.
- 686 Losh, J. L., Morel, F. M. M., and Hopkinson, B. M.: Modest increase in the C:N ratio of  
687 N-limited phytoplankton in the California Current in response to high CO<sub>2</sub>, *Mar.*  
688 *Ecol. Prog. Ser.*, 468, 31–42, 2012.
- 689 Losh, J. L., Young, J. N., and Morel, F. M.: Rubisco is a small fraction of total protein  
690 in marine phytoplankton, *New Phytol.*, 198, 52–58, 2013.
- 691 Luu-The, V., Paquet, N., Calvo, E., and Cumps, J.: Improved real-time RT-PCR method  
692 for high-throughput measurements using second derivative calculation and double  
693 correction, *Biotechniques*, 38, 287–293, 2005.
- 694 Mackey, M. D., Mackey, D. J., Higgins, H. W., and Wright, S. W.: CHEMTAX-a  
695 program for estimating class abundances from chemical markers: application to  
696 HPLC measurements of phytoplankton, *Mar. Ecol. Progr. Ser.*, 144, 265–283,  
697 1996.
- 698 Mackinder, L., Wheeler, G., Schroeder, D., Riebesell, U., and Brownlee, C.: Molecular  
699 mechanisms underlying calcification in coccolithophores, *Geomicrobiology*, 27,  
700 585–595, 2010.
- 701 Makino, A., Sakuma, H., Sudo, E., and Mae, T.: Differences between Maize and Rice in  
702 N-use efficiency for photosynthesis and protein allocation, *Plant Cell Physiol.*, 44,  
703 952–956, 2003.
- 704 Matsuda, Y., Nakajima, K., and Tachibana, M.: Recent progresses on the genetic basis  
705 of the regulation of CO<sub>2</sub> acquisition systems in response to CO<sub>2</sub> concentration,  
706 *Photosynth. Res.*, 109, 191–203, 2011.
- 707 Meakin, N. G., and Wyman, M.: Rapid shifts in picoeukaryote community structure in  
708 response to ocean acidification, *ISME J.*, 5, 1397–1405, 2011.
- 709 Meehl, G. A., Stocker, T. F., Collins, W. D., Friedlingsten, P., Gaye, A. T., Gregory, J.  
710 M., Kitoh, A., Knutti, R., Murphy, J. M., Noda, A., Raper, S. C. B., Watterson, I.

- 711 G., Weaver, A. J., and Zhao, Z. -C.: Global Climate Projections, in: Climate  
712 Change 2007 The Physical Science Basis, Contribution of Working Group I to the  
713 Fourth Assessment Report of the Intergovernmental Panel on Climate Change,  
714 Solomon, S., Qin, D., Manning, M., Chen, Z., Marquis, M., Averyt, K., Tignor, M.  
715 M. B., and Miller, H.L (EDs.), Cambridge University Press, United Kingdom and  
716 New York, 2007.
- 717 Michaels, A. F., and Silver, M. W.: Primary Production, sinking fluxes and the  
718 microbial food web, *Deep-Sea Res.* 35, 473–490, 1988.
- 719 Minoda, A., Weber, A. P. M., Tanaka, K., and Miyagishima, S.: Nucleus-independent  
720 control of the Rubisco operon by the plastid-encoded transcription factor Ycf30 in  
721 the red alga *Cyanidioschyzon merolae*, *Plant Physiol.*, 154, 1532–1540, 2010.
- 722 Obata, H., Karatani, H., and Nakayama, E.: Automated determination of iron in  
723 seawater by chelating resin concentration and chemiluminescence detection, *Anal.*  
724 *Chem.*, 65, 1524–1528, 1993.
- 725 Ondrusek, M. E., Bidigare, R. R., Sweet, S. T, Defreitas, D. A., and Brooks, J. M.:  
726 Distribution of phytoplankton pigments in the North Pacific Ocean in relation to  
727 physical and optical variability, *Deep-Sea Res.*, 38, 243-266, 1991.
- 728 Onoda, Y., Hikosaka, K., and Hirose, T.: Seasonal change in the balance between  
729 capacities of RuBP carboxylation and RuBP regeneration affects CO<sub>2</sub> response of  
730 photosynthesis in *Polygonum cuspidatum*, *J. Exp. Bot.*, 56, 755–763, 2005.
- 731 Pearson, P. N., and Palmer, M. R.: Atmospheric carbon dioxide concentration over the  
732 past 60 million years, *Nature*, 406, 659–699, 2000.
- 733 Pichard, S. L., Campbell, L., Kang, J. B., Tabita, F. R., and Paul, J. H.: Regulation of  
734 ribulose biphosphate carboxylase gene expression in natural phytoplankton  
735 communities 1. Diel rhythms, *Mar. Ecol. Progr. Ser.*, 139, 257–265, 1996.
- 736 Raven, J., Caldeira, K., Elderfield, H., Hoegh-Guldberg, O., Liss, P., Riebesell, U.,  
737 Shepherd, J., Turley, C., and Watson, A.: Ocean acidification due to increasing  
738 atmospheric carbon dioxide, The Royal Society policy document 12/05, Cardiff:  
739 Clyvedon Press, 2005.
- 740 Riebesell, U., Schulz, K. G., Bellerby, R. G. J., Botros, M., Fritsche, P., Meyerhöfer, M.,  
741 Neill, C., Nondal, G., Oschlies, A., Wohlers, J., and Zöllner, E.: Enhanced  
742 biological carbon consumption in a high CO<sub>2</sub> ocean, *Nature*, 450 (7169), 545–548,  
743 2007.
- 744 Riebesell, U., and Tortell, P. D.: Effects of ocean acidification on pelagic organisms and  
745 ecosystems, in: *Ocean acidification*, Gattuso, J.-P., and Hansson, L. (Eds.),  
746 Oxford University Press, New York, 83–98, 2011.
- 747 Rost, B., Riebesell, U., Burkhardt, S., and Sültemeyer, D.: Carbon acquisition of bloom  
748 forming marine phytoplankton, *Limnol. Oceanogr.* 48, 55–67, 2003.

- 749 Sabine, C. L., Feely, R. A., Gruber, N., Key, R. M., Lee, K., Bullister, J.L., Wanninkhof,  
750 R., Wong, C. S., Wallace, D. W. R., Tilbrook, B., Millero, F. J., Peng, T. -H.,  
751 Kozyr, A., Ono, T., and Rios, A. F.: The oceanic sink for anthropogenic CO<sub>2</sub>,  
752 Science, 305, 367–371, 2004.
- 753 Schloss, P. D., Westcott, S. L., Ryabin, T., Hall, J. R., Hartmann, M., Hollister, E. B.,  
754 Lesniewski, R. A., Oakley, B. B., Parks, D. H., Robinson, C. J., Sahl, J. W., Stres,  
755 B., Thallinger, G. G., Van Horn, D. J., and Weber, C. F.: Introducing mothur:  
756 open-source, platform-independent, community-supported software for describing  
757 and comparing microbial communities, Appl. Environ. Microbiol., 75, 7537–7541,  
758 2009.
- 759 Schoemann, V., Becquevort, S., Stefels, J., Rousseau, V., and Lancelot, C.: Phaeocystis  
760 blooms in the global ocean and their controlling mechanisms: a review, J. Sea  
761 Res., 53, 43–66, 2005.
- 762 Shannon, C. E.: A mathematical theory of communication, AT&T Teck. J., 27, 379–423,  
763 1948.
- 764 Shi, D., Xu, Y., Hopkinson, B. M., Morel, F. M. M.: Effect of ocean acidification on  
765 iron availability to marine phytoplankton, Science, 327, 676–679, 2010.
- 766 Simpson, E. H.: Measurement of diversity, Nature, 163, 688, 1949.
- 767 Singleton, D. R., Furlong, M. A., Rathbun, S. L., and Whitman, W. B.: Quantitative  
768 comparisons of 16S rRNA gene sequence libraries from environmental samples,  
769 Appl. Environ. Microbiol., 67, 4374–4376, 2001.
- 770 Smith, C. J., Nedwell, D. B., Dong, L. F., and Osborn, A. M.: Evaluation of quantitative  
771 polymerase chain reaction-based approaches for determining gene copy and gene  
772 transcript number in environmental samples, Environ. Microbiol., 8, 804–815,  
773 2006.
- 774 Springer, A. M., McRoy, C. P., and Flint, M. V.: The Bering Sea Green Belt: shelf-edge  
775 processes and ecosystem production, Fish. Oceanogr., 5, 205–223, 1996.
- 776 Stitt, M.: Rising CO<sub>2</sub> levels and their potential significance for carbon flow in  
777 photosynthetic cells, Plant Cell Environ., 14, 741–762, 1991.
- 778 Sugie, K., Endo, H., Suzuki, K., Nishioka, J., Kiyosawa, H., and Yoshimura, T.:  
779 Synergistic effects of *p*CO<sub>2</sub> and iron availability on nutrient consumption ratio of  
780 the Bering Sea phytoplankton community, Biogeosciences, 10, 6309–6321, 2013.
- 781 Suzuki, K., Kuwata, A., Yoshie, N., Shibata, A., Kawanobe, K., and Saito, H.:  
782 Population dynamics of phytoplankton, heterotrophic bacteria, and viruses during  
783 the spring bloom in the western subarctic Pacific, Deep-Sea Res. I, 58, 575–589,  
784 2011.
- 785 Suzuki, K., Minami, C., Liu, H., and Saino, T.: Temporal and spatial patterns of  
786 chemotaxonomic algal pigments in the subarctic Pacific and the Bering Sea  
787 during the early summer of 1999, Deep-Sea Res. II, 49, 5685–5704, 2002.



- 788 Takahashi, K., Fujitani, N., and Yanada, M.: Long term monitoring of particle fluxes in  
789 the Bering Sea and the central subarctic Pacific Ocean, 1990–2000, *Prog.*  
790 *Oceanogr.*, 55, 95–112, 2002.
- 791 Tortell, P. D., DiTullio, G. R., Sigman, D. M., and Morel, F. M. M.: CO<sub>2</sub> effects on  
792 taxonomic composition and nutrient utilization in an Equatorial Pacific  
793 Phytoplankton assemblage, *Mar. Ecol. Prog. Ser.*, 236, 37–43, 2002.
- 794 Tortell, P. D., Payne, C. D., Li, Y., Trimborn, S., Rost, B., Smith, W. O., Riesselan, C.,  
795 Dunbar, R. B., Sedwick, P., and DiTullio, G. R.: CO<sub>2</sub> sensitivity of Southern  
796 Ocean phytoplankton, *Geophys. Res. Lett.*, 35(4), L04605, 2008.
- 797 Trimborn, S., Brenneis, T., Sweet, E., and Rost, B.: Sensitivity of Antarctic  
798 phytoplankton species to ocean acidification: Growth, carbon acquisition, and  
799 species interaction, *Limnol. Oceanogr.*, 58, 997–1007, 2013.
- 800 Von Caemmerer, S. V., and Farquhar, G. D.: Some relationships between the  
801 biochemistry of photosynthesis and the gas exchange of leaves, *Planta*, 153, 376–  
802 387, 1981.
- 803 WMO.: Greenhouse gas bulletin: The state of greenhouse gases in the atmosphere based  
804 on global observations through 2012. World Meteorological Organization,  
805 Geneva, Switzerland, ISSN 2078–0796, 2013.
- 806 Wawrik, B., Paul, J. H., and Tabita, F. R.: Real-time PCR quantification of *rbcL*  
807 (ribulose-1,5-bisphosphate carboxylase/oxygenase) mRNA in diatoms and  
808 pelagophytes, *Appl. Environ. Microbiol.*, 68, 3771–3779, 2002.
- 809 Welschmeyer, N. A.: Fluorometric analysis of chlorophyll *a* in the presence of  
810 chlorophyll *b* and pheopigments, *Limnol. Oceanogr.*, 39, 1985–1992, 1994.
- 811 Wright, S. W., and van den Enden, R. L.: Phytoplankton community structure and  
812 stocks in the east Antarctic marginal ice zone (BROKE survey, January–March  
813 1996) determined by CHEMTAX analysis of HPLC pigment signature, *Deep-Sea*  
814 *Res. II*, 47, 2363–2400, 2000.
- 815 Xu, H. H., and Tabita, F. R.: Ribulose-1,5-bisphosphate carboxylase/oxygenase gene  
816 expression and diversity of lake Erie planktonic microorganisms, *Appl. Environ.*  
817 *Microbiol.*, 62, 1913–1921, 1996.
- 818 Yoshimura, T., Nishioka, J., Suzuki, K., Hattori, H., Kiyosawa, H., Watanabe, Y.:  
819 Impacts of elevated CO<sub>2</sub> on organic carbon dynamics in nutrient depleted Okhotsk  
820 Sea surface waters, *J. Exp. Mar. Biol. Ecol.*, 395, 191–198, 2010.
- 821 Yoshimura, T., Sugie, K., Endo, H., Suzuki, K., Nishioka, J., and Ono, T.: Organic  
822 matter production response to CO<sub>2</sub> increase in open subarctic plankton  
823 communities: Comparison of six microcosm experiments under iron-limited  
824 and-enriched bloom conditions, *Deep-Sea Res. I*, 94, 1–14, 2014.
- 825 Yoshimura, T., Suzuki, K., Kiyosawa, H., Ono, T., Hattori, H., Kuma, K., and Nishioka,  
826 J.: Impacts of elevated CO<sub>2</sub> on particulate and dissolved organic matter

827 production: Microcosm experiments using iron deficient plankton communities in  
828 open subarctic waters, *J. Oceanogr.*, 69, 601–618, 2013.

829 **Table 1.** Carbonate chemistry, nutrients, and Fe parameters (value  $\pm$  1 standard  
830 deviation,  $n = 3$ ) during the incubation experiment. Carbonate parameters are the initial  
831 and mean values throughout the incubation. Macronutrients and Fe parameters are the  
832 values at the initial or final sampling days (i.e., day 5 for the control and day 6 for the  
833 Fe-added treatments). Standard deviation was not assessed for initial TD-Fe  
834 concentration because samples were collected from single source. See figures S1 and S2  
835 for the complete data set.  
836

	DIC ( $\mu\text{mol kg}^{-1}$ )	TA ( $\mu\text{mol kg}^{-1}$ )	$p\text{CO}_2$ ( $\mu\text{atm}$ )	$\text{CO}_2$ ( $\mu\text{mol kg}^{-1}$ )	pH (Total scale)
C-Initial	2086.4 $\pm$ 2.8	2249.1 $\pm$ 5.0	388.4 $\pm$ 18.1	18.4 $\pm$ 0.9	8.05 $\pm$ 0.02
C-380	2075.5 $\pm$ 8.1	2252.9 $\pm$ 10.8	355.7 $\pm$ 34.7	16.8 $\pm$ 1.6	8.09 $\pm$ 0.04
C-600	2151.6 $\pm$ 7.8	2250.9 $\pm$ 4.7	604.1 $\pm$ 36.2	28.5 $\pm$ 1.7	7.88 $\pm$ 0.02
Fe-Initial	2085.3 $\pm$ 0.8	2250.0 $\pm$ 4.9	383.4 $\pm$ 12.6	18.1 $\pm$ 0.6	8.06 $\pm$ 0.01
Fe-180	1959.9 $\pm$ 62.0	2244.1 $\pm$ 16.0	202.0 $\pm$ 50.9	9.5 $\pm$ 2.4	8.21 $\pm$ 0.10
Fe-380	2068.5 $\pm$ 27.7	2235.7 $\pm$ 14.9	375.9 $\pm$ 47.9	17.8 $\pm$ 2.3	8.01 $\pm$ 0.05
Fe-600	2120.6 $\pm$ 33.5	2248.5 $\pm$ 12.0	512.6 $\pm$ 135.5	24.2 $\pm$ 6.4	7.96 $\pm$ 0.11
Fe-1000	2200.2 $\pm$ 12.6	2248.4 $\pm$ 9.8	913.8 $\pm$ 159.8	43.2 $\pm$ 7.6	7.72 $\pm$ 0.07

837  
838 **Table 1.** (Continued)  
839

	Nitrate ( $\mu\text{mol L}^{-1}$ )	Phosphate ( $\mu\text{mol L}^{-1}$ )	Silicic acid ( $\mu\text{mol L}^{-1}$ )	TD-Fe ( $\text{nmol L}^{-1}$ )
C-Initial	18.06 $\pm$ 0.10	1.47 $\pm$ 0.01	16.95 $\pm$ 0.12	1.35
C-380	7.09 $\pm$ 0.27	0.65 $\pm$ 0.02	0.28 $\pm$ 0.05	0.27 $\pm$ 0.03
C-600	12.01 $\pm$ 0.27	0.98 $\pm$ 0.02	3.04 $\pm$ 0.32	0.29 $\pm$ 0.04
Fe-Initial	18.09 $\pm$ 0.11	1.47 $\pm$ 0.01	16.90 $\pm$ 0.12	5.50 $\pm$ 0.10
Fe-180	0.13 $\pm$ 0.04	0.10 $\pm$ 0.01	0.66 $\pm$ 0.09	4.60 $\pm$ 0.19
Fe-380	0.09 $\pm$ 0.00	0.12 $\pm$ 0.04	0.50 $\pm$ 0.01	4.48 $\pm$ 0.12
Fe-600	0.08 $\pm$ 0.00	0.10 $\pm$ 0.00	0.50 $\pm$ 0.01	4.34 $\pm$ 0.08
Fe-1000	0.08 $\pm$ 0.00	0.08 $\pm$ 0.02	0.47 $\pm$ 0.02	4.18 $\pm$ 0.24

840

841 **Table 2.** Number of OTUs, richness index, and diversity indices (value  $\pm$  95%  
 842 confidence interval) for *rbcL* cDNA libraries obtained from the initial seawater and the  
 843 incubation bottles on day 2 (Fe-380 and Fe-600) and day 3 (C-380 and C-600).  
 844

Library	No. of sequences	No. of OTUs	Chao1	$H'$	$D$
Initial	35	10	25.0	1.81 $\pm$ 0.32	0.197 $\pm$ 0.086
C-380	50	15	20.0	1.98 $\pm$ 0.36	0.232 $\pm$ 0.110
C-600	50	14	29.0	1.60 $\pm$ 0.41	0.369 $\pm$ 0.148
Fe-380	50	13	23.0	2.24 $\pm$ 0.23	0.116 $\pm$ 0.042
Fe-600	50	12	19.5	2.01 $\pm$ 0.26	0.158 $\pm$ 0.053

845

846 **Table 3.** Significance levels for differences among *rbcL* cDNA libraries as calculated  
 847 with LIBSHUFF. *p* values < 0.05 are bolded.  
 848

	Library (Y)				
	Initial	C-380	C-600	Fe-380	Fe-600
Library (X)					
Initial	—	0.434	0.573	0.383	0.587
C-380	0.153	—	0.086	0.101	0.898
C-600	0.523	0.500	—	<b>0.004</b>	0.033
Fe-380	<b>&lt;0.001</b>	<b>&lt;0.001</b>	<b>&lt;0.001</b>	—	<b>0.002</b>
Fe-600	<b>0.009</b>	<b>0.004</b>	<b>&lt;0.001</b>	0.030	—

849

850 **Figure captions**

851

852 **Figure 1.** Temporal changes in fucoxanthin (a and b) and 19'-hexanoyloxyfucoxanthin  
853 (c and d) concentrations. Left (a and c) and right graphs indicate data from  
854 the control and Fe-added treatments, respectively. Error bars denote  $\pm 1$   
855 standard deviation (SD,  $n = 3$ ). Standard deviations were not assessed on  
856 days 2 (Fe-added treatments) and 3 (control treatments) because samples were  
857 collected from each single bottle.

858

859 **Figure 2.** Mean contributions of each phytoplankton group to total Chl *a* biomass  
860 estimated by CHEMTAX in the (A) control bottles at 380 and 600 ppm CO<sub>2</sub>,  
861 and (B) Fe-added bottles at 180, 380, 600 and 1000 ppm CO<sub>2</sub> ( $n = 1$  or 3).

862

863 **Figure 3.** Relationship between fucoxanthin concentration and diatom-specific *rbcL*  
864 copy number ( $y = 7.62 \times 10^8 x + 1.90 \times 10^8$ ,  $r^2 = 0.677$ ,  $p < 0.001$ ,  $n = 28$ ).

865

866 **Figure 4.** Abundances of *rbcL* mRNA (cDNA) normalized to *rbcL* gene copy number  
867 (*rbcL* cDNA/DNA) in the control bottles on day 3 and the Fe-added bottles  
868 on day 2. Open bars and closed bars denote control and Fe-added treatments,  
869 respectively. Error bars indicate  $\pm 1$  SD ( $n = 3$ ).

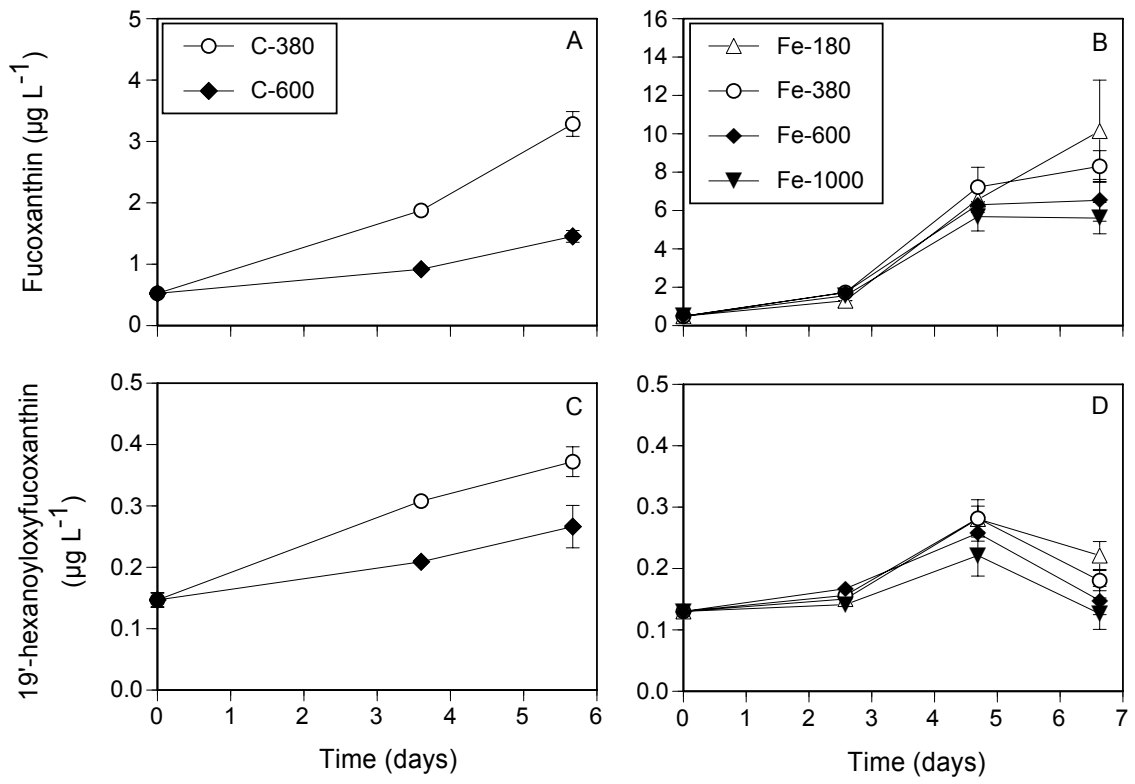
870

871 **Figure 5.** Rarefaction analysis of the diatom-specific *rbcL* clone libraries. The  
872 rarefaction curves, plotting the number of operational taxonomic units  
873 (OTUs) as a function of the number of sequences, were computed by the  
874 software mothur. C and Fe indicate the control and Fe-added treatments,  
875 respectively.

876

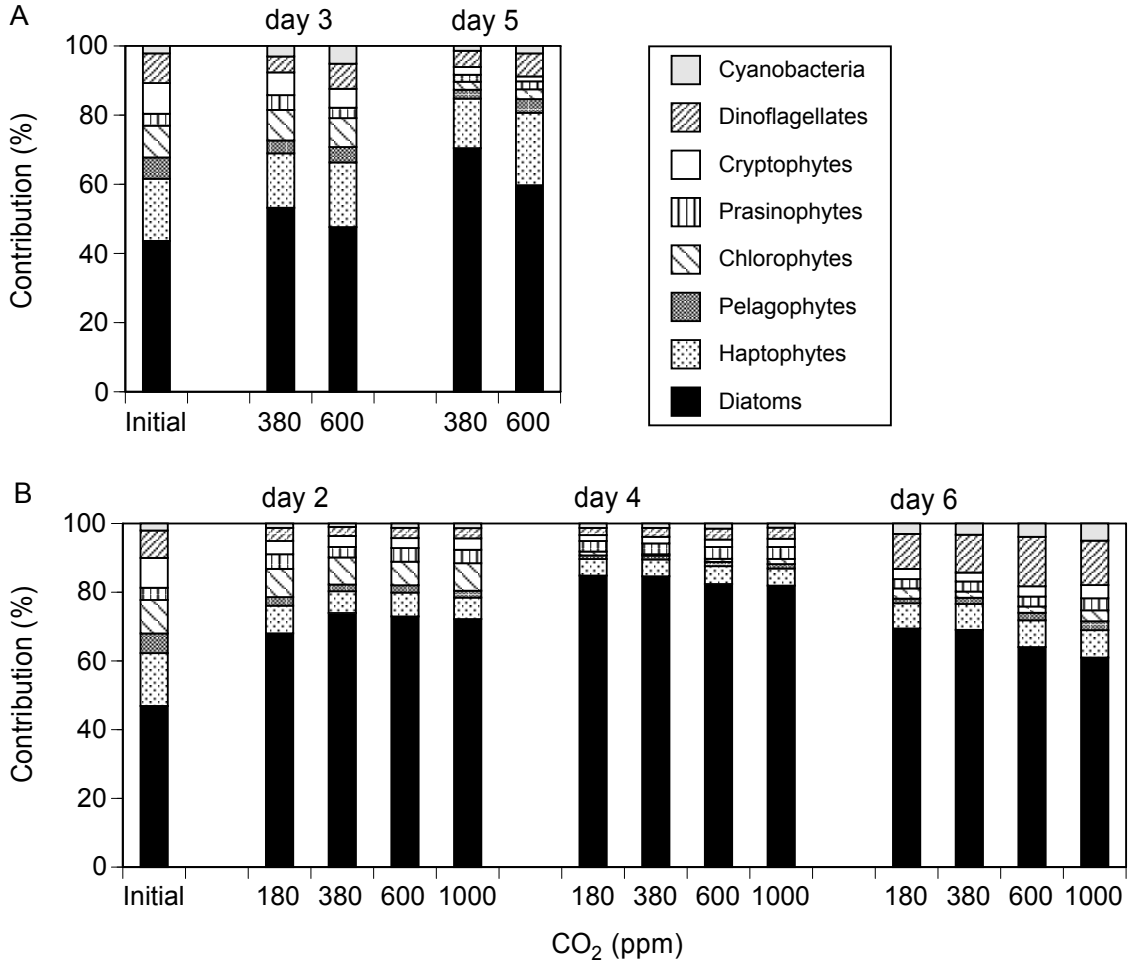
877 **Figure 6.** Relative phylotype contributions in the *rbcL* cDNA libraries obtained from  
878 the initial seawater and the incubation bottles at day 2 (Fe-380 and Fe-600)  
879 and day 3 (C-380 and C-600).

880



881

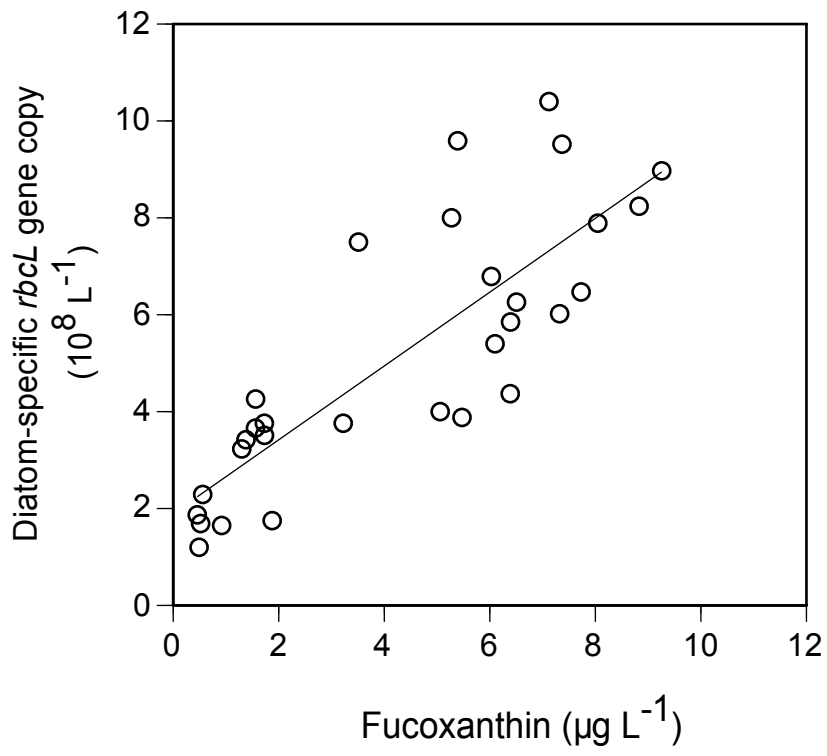
882 **Figure 1**



883

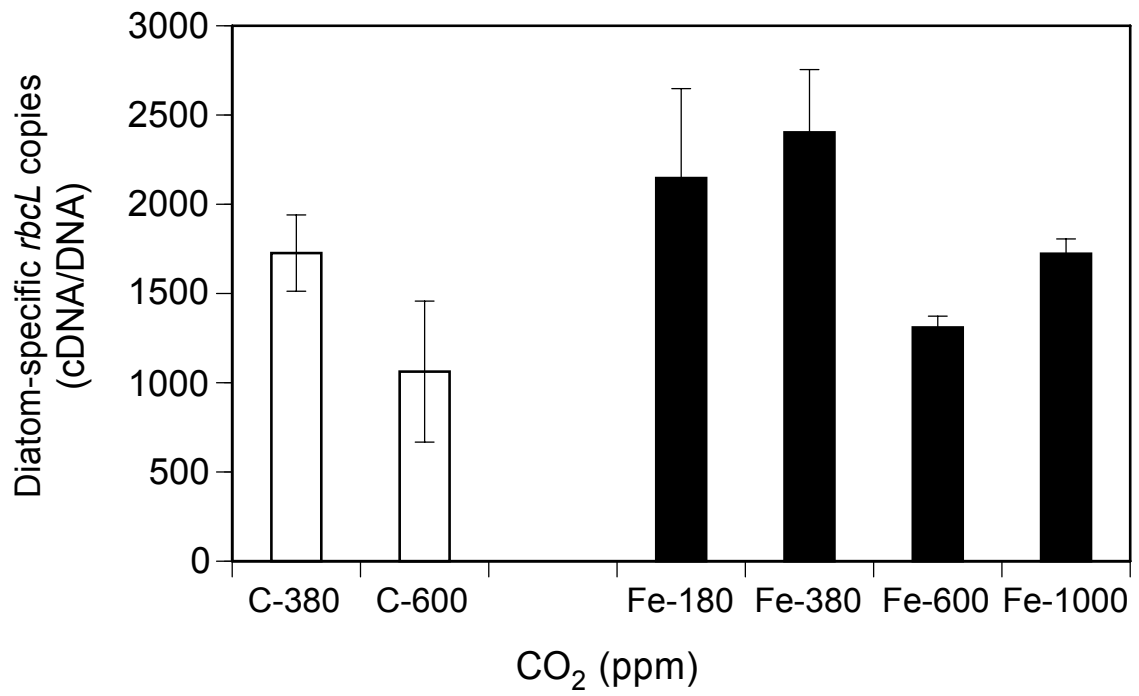
884 **Figure 2**





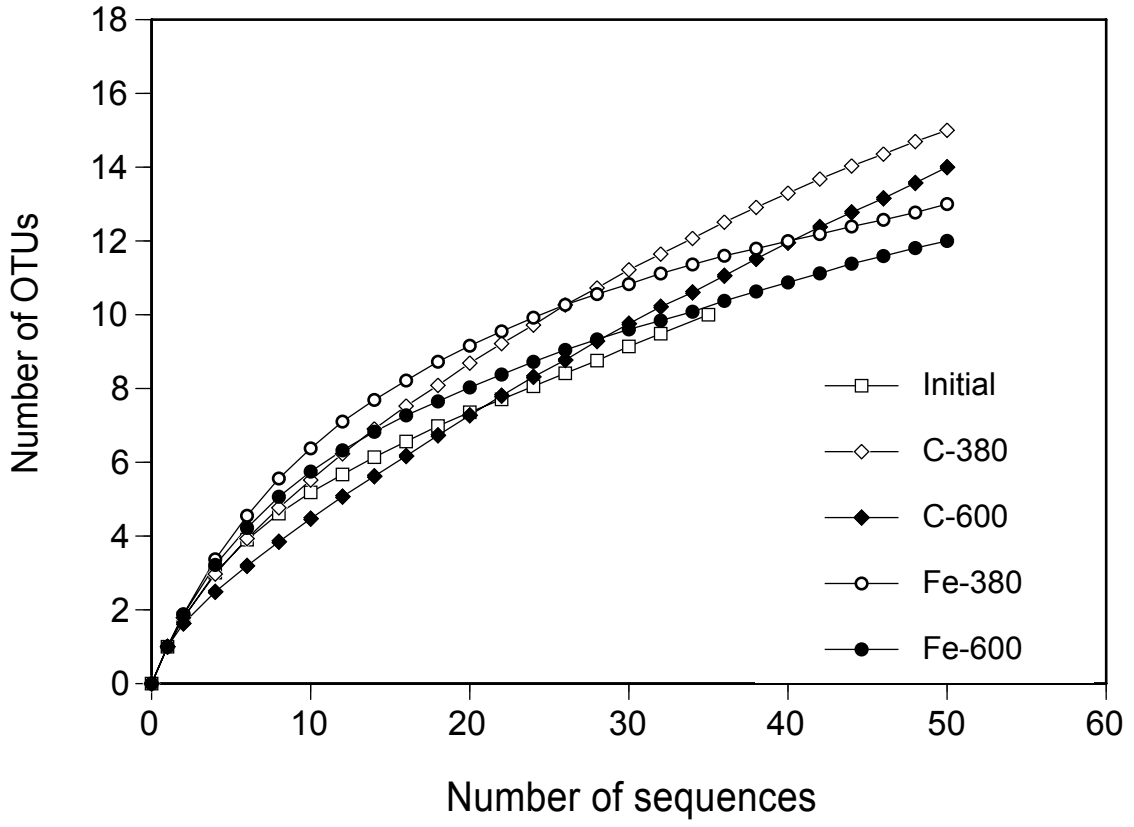
885

886 **Figure 3**



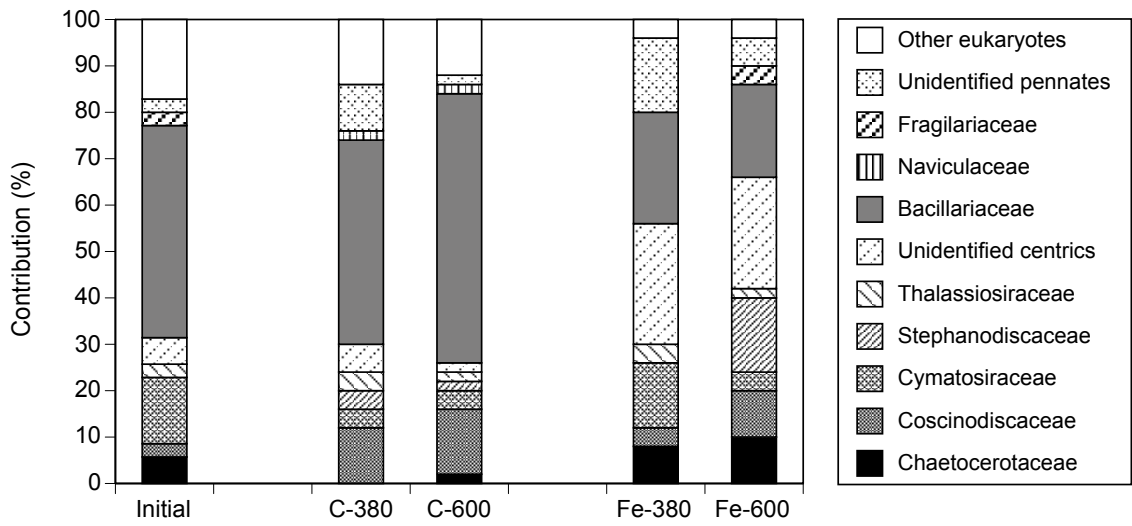
887

888 **Figure 4**



889

890 **Figure 5**



891

892 **Figure 6**